Journal of Clinical & Experimental Cardiology

Entin-Meer et al., J Clinic Experiment Cardiol 2012, 3:3
DOI: 10.4172/2155-9880.1000184

Research Article Open Access

Renal Failure is Associated with Driving of Gene Expression towards Cardiac Hypertrophy and Reduced Mitochondrial Activity

Michal Entin-Meer[1], Metsada Pasmanik-Chor[2], Jeremy Ben-Shoshan[1], Sofia Maysel-Auslender[1], Pavel Goryainov[1], Ido Laron[1], Shelly Klipper[1], Varda Oron-Karni[2], Jonathan Semo[1,3], Einat Hertzberg[1,4] and Gad Keren[1,3]*

[1]*The Laboratory of Cardiovascular Research, Department of Cardiology, Tel-Aviv Sourasky Medical Center, Israel*
[2]*The Bioinformatics Unit, G.S.W. Faculty of Life Sciences, Tel-Aviv University, Israel*
[3]*The Department of Medicine, Sackler School of Medicine, Tel-Aviv University, Israel*
[4]*The Department of Physiology and Pharmacology, Sackler School of Medicine, Tel-Aviv University, Israel*

Abstract

Background: The clinical concomitant presentation of cardiac and renal failure (RF) has been referred to as the "cardiorenal syndrome" (CRS), whereby acute or chronic dysfunction of one organ induces acute or chronic dysfunction of the other. To improve our understanding of the cellular and molecular mechanisms underlying the development and diversification of CRS we established a model for CRS and studied the unique gene expression patterns associated with this syndrome.

Methods and Results: We have utilized a rat model in which an acute myocardial infarction (AMI) was induced on the background of subtotal nephrectomy. Changes in cardiac functions and gene expression were analyzed as detailed below. The data demonstrate that chronic RF (CRF) enhances fibrosis of the cardiac tissue. The gene chip array data detect overexpression of genes associated with hypertrophy as well as to reduced mitochondrial activity in the heart. The gene chip data also indicate that chymase inhibitors and coenzyme Q10 may be beneficial in the management of RF- induced cardiac hypertrophy. We further show that in line with the upregulation of the Ngal gene, LCN2, upon acute MI and CRS, Ngal protein levels significantly increase five days post infarction and remain stably elevated when the cardiac disease progresses to CRS.

Conclusions: Acute cardiac injury in the setting of CRF is associated with marked histological and gene expression changes in the heart. Based on our data, predictive biomarkers for the development of RF- induced cardiac hypertrophy as well as novel therapeutic directions may emerge.

Keywords: Cardiorenal syndrome (CRS); Chronic renal failure (CRF); Cardiac hypertrophy

Introduction

Concomitant cardiac and renal dysfunction, termed cardiorenal syndrome (CRS) where acute or chronic impairment of one organ aggravates dysfunction of the other organ has been thoroughly described [1]. Five types of clinically relevant CRS were described according to the chronicity or abruptness of the development of the syndrome [2] and are all associated with serious outcomes. Impaired renal function, even when mild, represents a major risk factor for cardiovascular disease and significantly affects the long term outcome of the patients [3]. In acute myocardial infarction (AMI) leading to heart failure (HF), a preexisting impaired renal function represents an adverse prognostic indicator for deterioration of the cardiac function. Multiple pathophysiologic mechanisms have been implicated in this crosstalk between organs and the associated progression of the disease both in the kidney and in the heart [1,2]. ACE inhibitors and angiotensin receptor blockers have protective effects on the heart and the kidney when function is impaired. Other approved treatment modalities include beta blockers and the implantation of CRT to improve cardiac synchronization and function.

Van Dokkum et al. [4] and his colleagues established a model in rats where renal dysfunction is induced by unilateral nephrectomy and cardiac dysfunction by coronary artery ligation. In another study, in which MI was induced one week post subtotal nephrectomy (STN), the authors have demonstrated protective role for ACE inhibitors or ACE/NEP (neutral endopeptidase) inhibitors in reducing renal damage [5]. In the same model the group has recently shown that renal failure causes excessive shortening of cardiac telomeres after MI suggesting that genetic modification may underlie the mutual interaction of kidney and heart dysfunction [6].

Numerous groups as well as our laboratory have explored new approaches including enhancement of cardioprotective and regenerative properties of the heart. These two modalities were successfully integrated through genetic modification of stem cells to ameliorate myocyte regeneration as well as angiogenic capacities [7-8]. Additional research is required to elucidate the processes that underlie cardiac and renal dysfunction in order to explore potential treatment modalities.

In the current study we sought to assess alterations in gene expression which may contribute to cardiac dysfunction upon CRF and CRS. Deep understanding of the underlying mechanisms may deliver rational interventions (pharmacological or genetic) which may improve clinical treatment of CRS patients, and improve their prognosis.

***Corresponding author:** Gad Keren, MD, Department of Cardiology, Tel-Aviv Sourasky Medical Center, Tel-Aviv, 64239 Israel, Tel: 972-3-6974762; Fax: 972-3-6974808; E-mail: kereng@tasmc.health.gov.il

Received March 11, 2012; **Accepted** March 28, 2012; **Published** March 31, 2012

Citation: Entin-Meer M, Pasmanik-Chor M, Ben-Shoshan J, Maysel-Auslender S, Goryainov P, et al. (2012) Renal Failure is Associated with Driving of Gene Expression towards Cardiac Hypertrophy and Reduced Mitochondrial Activity. J Clinic Experiment Cardiol 3:184. doi:10.4172/2155-9880.1000184

Materials and Methods

Rat model for CRS

Experimental protocol was approved by the IRB committee for animal experimentation at the Tel Aviv Medical Center and conforms to the Guide for the Care and Use of Laboratory Animals published by the US National Institutes of Health. The model was based on a previously described model with several changes [5]. Briefly, male Lewis rats underwent subtotal nephrectomy (STN) in two subsequent surgeries: 2/3 of the left kidney was removed initially, followed by removal of the right kidney one week later. Four weeks afterwards the animals were orally intubated and artificially ventilated with a respirator (Harvard apparatus). MI was induced by ligation of the left anterior descending (LAD) coronary artery after chest opening. Prior to the surgical procedures animals were anesthetized with a mixture of ketamine (50 mg/Kg) and xylazine (10 mg/ml) by an intraperitoneal injection. The animals were terminated on the following day by CO_2 inhalation according to the IRB guidelines. The analyses for the MI and CRS groups were performed only on animals in which the echocardiography study confirmed fractional shortening (FS) ranging from 15-28%, which is associated with moderate to severe left ventricular dysfunction (LVD). The experimental design included 4 arms: sham-operated (where the abdomen was cut-open twice in parallel to the time points of the two subsequent STN surgeries and four weeks later the chest was opened and closed in parallel to MI induction in the relevant animals), STN, MI and STN + MI. For the assessment of gene expression alteration, animals were sacrificed 5 days only after MI induction in order to monitor genes within the acute phase which takes place after AMI (in this experiment the MI was confirmed by visualization only). The time frame for each experimental group is outlined in Figure 1 A and B. We started the experiment with n = 15/ arm and after the 3 phase surgeries 8-10 animals survived in each experimental group.

Assessment of cardiac function

Thirty days post LAD ligation, animals were anesthetized with ketamine (40 mg/Kg) and xylazine (8 mg/Kg) and transthoracic echocardiography was performed by use of an Acuson XP-10 cardiac ultrasound machine with a 15-MHz transducer, which has 128 imaging elements configured in a phased-array format in order to assess cardiac function.

Laboratory of RF

Renal failure was confirmed by creatinine (Cr) clearance test (CCT) and sera BUN levels. CCT was calculated using the following equation: [Cr (urine)/Cr (serum)*urine volume]/1440. In addition, urine Ngal levels were determined in all experimental groups using an ELISA kit according to the manufacturer's instructions (Bioporto Diagnostics, Denmark).

Histological assessment of cardiac and renal damage

The left ventricles (LV) were fixed with 4% paraformaldehyde and sliced into transverse sections and paraphinyzed. The slices were sectioned (5 μm) and stained with Masson's trichrome. Photos were taken by Nicon camera using the NIS-elements 3.0 software. All sections were evaluated by a pathologist, blinded to the protocol design.

RNA isolation, amplification, labeling and hybridization to DNA chip arrays

RNA from the cardiac tissue of 4 research arms: sham, STN, MI (day 5 after LAD ligation) and STN+ MI were extracted by phenol/chloroform (Biological industries) and tested for purity by nanodrop and agarose gel electrophoresis. Four samples derived from each one of the 4 arms were divided to two pools of two RNA samples so that the reactions were started with two pools of two RNA samples in each group (8 samples total). RNA samples were reverse transcribed followed by amplification and hybridization steps. For details see Supplementary Methods 1 in "Supplemental file".

Quantitative Real-Time (RT) PCR

Total RNA was extracted from the harvested hearts by phenol/chloroform/isoamyl alcohol (Biological Industries, Israel). For gene expression studies, 1 μg RNA was transcribed using Verso™ RT-PCR Kits (ABgene, USA). For miRNA RT analysis, 25ng of RNA were transcribed using universal LNATM cDNA synthesis kit (Exiqon, Denmark). A quantitative PCR was performed with the Syber Green PCR kit (Invitrogen, Israel). Primers used for real-time analysis are listed in Supplemental Methods 2 in "Supplemental file".

Statistical analysis: Differences in mean values between groups were compared by one way ANOVA followed by Scheffe's post hoc test, or by two-tailed student's t-test unless otherwise specified. In all tests, $P < 0.05$ was considered statistically significant.

Results

Cardiac echocardiography and histology point out to CRF-induced cardiac hypertrophy

Following a 9- week experimental period as outlined in Figure 1A the animals were terminated. Prior to termination we calculated the CCT values which, as expected, were significantly lower following

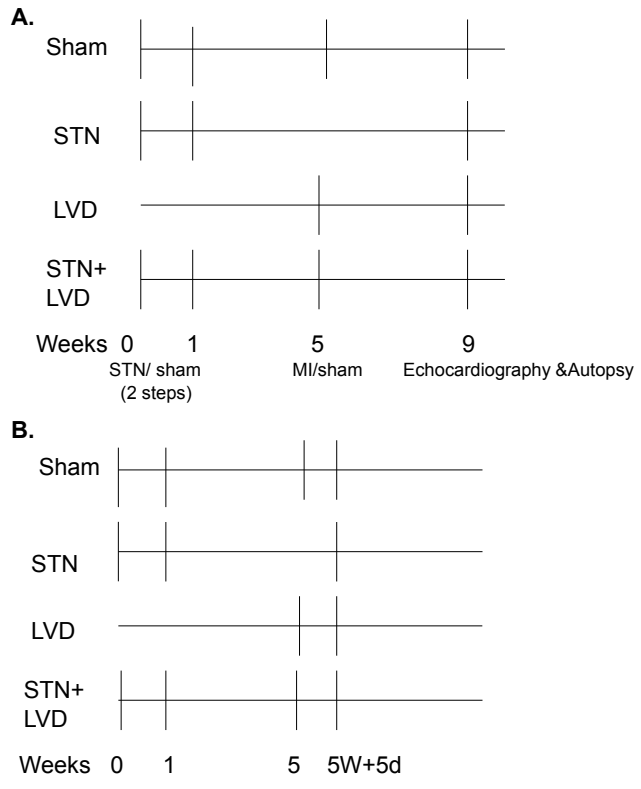

Figure 1: Experimental protocol-time course.

STN, compared to controls (data not shown). An echocardiography scan confirmed a moderate to severe LVD in animals which underwent LAD ligation (FS ranging from- 15-28%). In the CRF group, however, cardiac function was not affected and the fractional shortening values which were similar to those of the sham-operated controls (FS>40, data not shown), suggesting that cardiac changes occurring upon kidney injury are not detrimental to induce LVD.

Upon termination, the hearts and the remaining kidney stumps were collected. Representative photos show the collapsed and enlarged left ventricle in CRS animals (left, STN+MI) compared to sham (right) (Figure 2A), and a significantly hypertrophic kidney stump, compared to sham-operated control animals (Figure 2B). A representative stain of the LV section performed four weeks following acute MI is given in Figure 2C, demonstrating a massive fibrotic area at the infracted zone as expected. Notably, the histological examination using Masson's trichrome staining revealed interstitial fibrosis in 4 out of 5 LV sections of STN animals (a representative photo is given Figure 2D) with no similar cardiac fibrosis in the sham-operated animals (not shown). In line with the histological data, the heart weight per body weight ratio was higher upon all experimental groups compared to sham (heart/body of sham =0.37 ± 0.009) (Figure 2E). The weight ratios compared to sham were significantly elevated upon STN+AMI (5 days post MI)

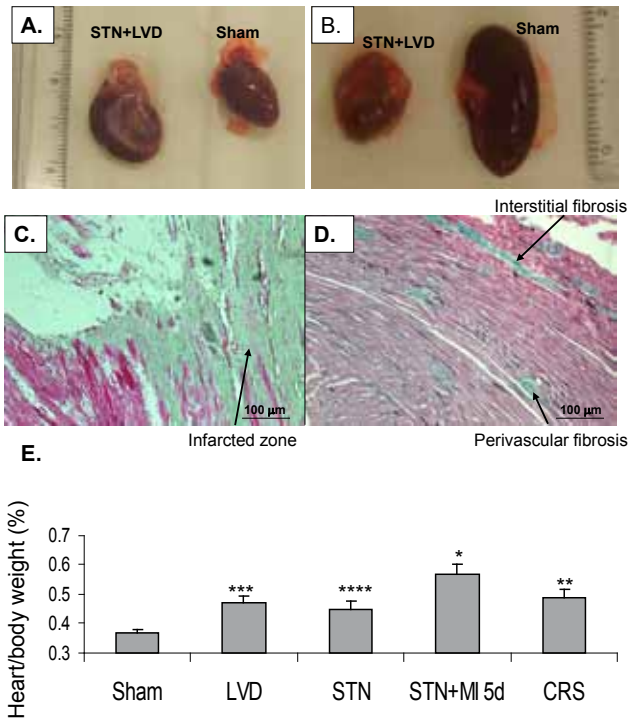

Figure 2: Cardiac and renal remodeling in CRS upon termination. (A) A representative overview of an infracted heart in CRS (STN+MI) versus sham-operated heart; (B) The remaining left kidney stump in a representative CRS animal versus normal (sham-operated) kidney. All animals were terminated 8 weeks post STN (4 weeks post MI induction). A histological analysis using Masson's trichrome is shown for LV sections upon MI (C) or STN (D). The graph in panel E shows the ratios of heart weight to body weight (in percentage). CHF stands for MI 4 weeks. (*) p (STN+MI) < 0.008 compared to sham, STN and CHF (no statistical significance compared to CRS, p=0.24). (**) p (CRS)=0.014 compared to sham a (no significance compared to the other groups, p>0.2). (***) p (CHF)= 0.056 compared to sham and (****) p (STN) compared to sham= 0.139, showing a trend towards statistical significance (one way ANOVA).

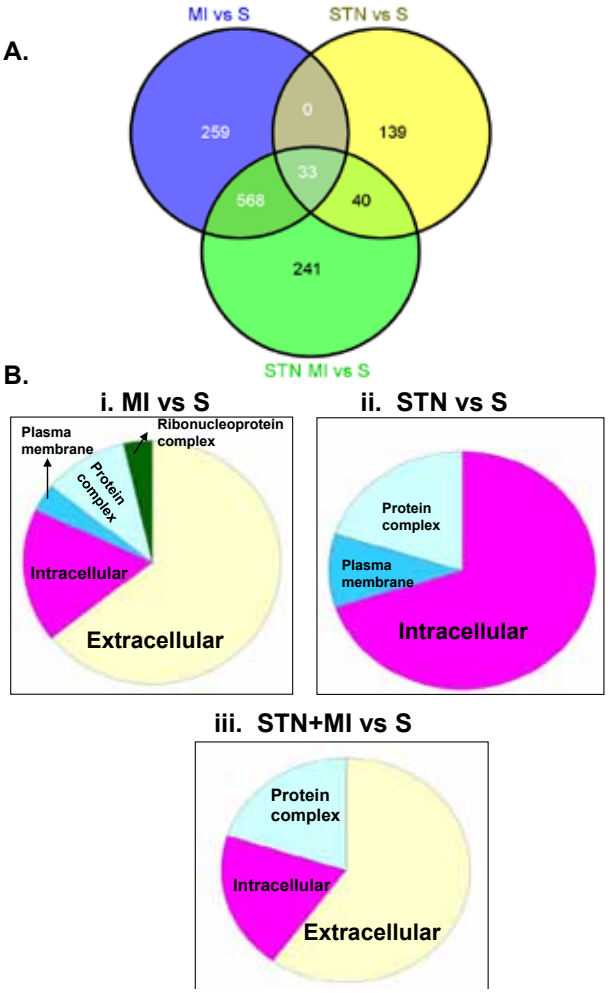

Figure 3: An overview on the cardiac genes whose expression is modified upon STN, acute MI or STN+MI (all compared to sham). (A) Venn diagram which includes differentially expressed genes upon STN, MI or STN+MI compared to sham (fold change >+1.5 or <-1.5 and p<0.05) (B) Pie charts representing the enriched cellular components of the modified genes (i. MI vs Sham; ii. STN vs Sham; iii. STN+MI vs Sham) according to Panther database (http://www.pantherdb.org/).

(heart/body= 0.57 ± 0.03, p=0.0001) and upon CRS (0.49 ± 0.03, p= 0.01. Similarly, the weight ratio of LVD (4 weeks post MI) and the CRF groups were higher compared to sham with a trend towards statistical significance (heart/body=0.47 ± 0.02, p=0.057 and heart/body=0.45 ± 0.03, p=0.13 in the LVD and STN groups, respectively). The data, thus, point out that CRF per se may lead to cardiac hypertrophy.

Alterations in the cardiac gene expression patterns are associated with cardiac hypertrophy

In order to study which genes could account for the pathological cardiac fibrosis and hypertrophy, we applied a gene chip array analysis on RNA samples isolated from the whole cardiac tissue following: acute MI, CRF (STN), CRS (STN+acute MI) and sham operations. The time frame for this experimental design is outlined in Figure 1B. The complete differentially expressed gene lists are given in Supplemental file Table 1. Interestingly, Venn diagram, crossing between the 3 differentially expressed gene-lists compared to sham, revealed only

33 common genes. No further genes were common to MI and STN (lists compared to sham). On the other hand, 568 genes (approximately 70% of the genes) were common to MI and STN+MI (Figure 3A). Our analysis points out to different biological cascades initiated in the cardiac tissue upon MI or STN; while the STN+MI and MI genelists harbor similar biological networks. A list of genes which may be most relevant to cardiac structure and function was made for each treatment (Tables 1, 2 and 3 for MI, STN and STN+MI versus sham, respectively) based on best differential expressed genes and affiliated KEGG annotations which relate to cardiac structure or function. All further analyses described below were based on these 3 lists of selected genes.

Most of the genes modified upon MI or STN+MI encode proteins acting at the extracellular environment (Figure 3Bi and 3Biii), while the vast majority of the genes modified upon CRF encode proteins located at the intracellular compartment (Figure 3Bii).

Next, the main molecular pathways modified upon STN, MI or the combined condition STN+MI, were analyzed using five independent gene ontology web-tools. These are shown in Supplemental Table 2. The up-regulated genes modified upon acute MI are related to the following biological pathways: ECM proteolysis, cell adhesion, complement cascades, angiogenesis, inflammation and apoptosis (See differentially expressed gene clustering Figure 4A, Table 1 and Supplementary Table 2 in "Supplemental file").

Functional annotation of the genes whose expression was significantly changed in the STN gene-list compared to sham revealed two major gene clusters (Figure 4B and Table 2). The first cluster of up-regulated genes (red) includes mainly genes which are affiliated with ribosome biogenesis and translational elongation. Numerous ribosomal genes were quantified to be upregulated compared to sham by real-time (RT) PCR analysis, among which the upregulation of RPS11, RPS19 and RPS23 was statistically significant (+2.0-3.0, $p<0.05$, Figure 5A). The enhanced translation is probably accompanied by an increase in DNA synthesis as reflected by the somewhat non-significant upregulation of several nucleosomal histone genes (Table 2, Figures 4B and 5A). The other major gene cluster, was dramatically downregulated upon STN (blue), and includes genes which are mainly affiliated with proteolysis and proteosome biosynthesis, including the proteosomal genes psma1, psma3, psma4 and psmd6 (Figure 4B and Table 2). Psma3 downregulation was significantly validated by RT analysis (Figure 5B). Three additional genes or gene families belonging to this cluster are (Figure 3B, blue, and Table 1): 1. Rab2a, Rab3ip, Rab10, Rab14 and Rab21. These RAS-related GTPases function in apoptotic cell removal by enhancing phagosome maturation [10]. The downregulation of Rab14 was confirmed by RT analysis (Figure 5B). 2. A set of several rat mast cell proteases, which are also known as rat chymases. Out of these, it is worthwhile mentioning MCPT2 which was downregulated by fold-change (FC) of 4.4 compared to sham ($p=0.07$) and confirmed by real-time analysis (Figure 5B). 3. Complement factor 3 (C3) which was downregulated upon STN (significantly confirmed in RT analysis) (Figure 5B), while upon MI or STN+MI, C3 expression was significantly upregulated (Supplemental Table 1).

Taken together, the gene chip analysis suggests an increased synthesis of ribosomal proteins which is accompanied by a marked decrease in intracellular proteolytic activities. These processes may culminate in cardiac hypertrophy which takes place upon CRF.

Gene ontology	**Gene full name/Function**	**Gene symbol** (fold-change and p-value)
ECM proteolytic activity, Collagen formation & focal adhesion	collagen, procollagen C-endopeptidase enhancer, Lysis oxidase, collagen triple helix repeat containing 1, fibrillin, fibronectin, versican, hyaluronic acid (HA) receptor, Metalloproteinase, EGF containing fibulin-like extracellular matrix protein 2, elastin, spondin 1, extracellular matrix protein, lumican, fibroblast growth factor 9, Tissue growth factor, periostinosteoblast specific factor	Col1a1 (5.36, 0.0001), Col5a1 (3.65, 0.0006), Col5a2 (4.84, 0.0004), Col4a1 (3.61, 0.01), Col6a3 (3.64, 0.01), Col1a2 (4.20, 0.0003), Col3a1 (4.08, 0.0006), Pcolce (4.05, 0.003), Loxl1 (3.27, 0.0037), Cthrc1 (6.17, 0.0005), Fbn1 (4.45, 0.0002), Fn1 (4.83, 0.0005), Vcan (3.63, 0.0001), CD44 (1.83, 0.0031), MMP14 (3.82, 0.0012), MMP19 (2.19, 0.0011), MMP23 (2.38, 0.0022), Timp1 (7.40, 0.0049), Efemp2 (3.36, 0.0031), Eln (3,21, 0.0016), Spon1 (3.37, 0.0007), Lum (2.57, 0.0179), FGF9 (-1.61, 0.0414), CTGF (3.07, 0.0015), TGFb1 (1.50, 0.0315), Postn (14.94, 0.00001)
Complement Cascades & Immune response	Complement factor, Integrin alpha, leukocyte immunoglobulin-like receptor, Fc fragment of IgG, colony stimulating factor 2 receptor, beta	C3ar1 (2.75, 0.0028), C3 (4.13, 0.0164), C6 (2.99, 0.0112), C1r (2.08, 0.0193), C2 (2.72, 0.0410), Itgam (3.82, 0.001), Lilrb4 (3.20, 0.0009), Fcgr1a (3.23, 0.0029), Csf2rb (3.33, 0.0124)
Blood vessel formation & angiogenesis	tubulin, beta 6, Heme oxigenase, Cys-rich angiogenic inducer 61, alanyl aminopeptidase	Tubb6 (3.29, 0.0076), Hmox1 (6.99, 0.0001), Cyr61 (3.30, 0.0283), Anpep (4.05, 0.0003)
Muscle contraction & Ca^{2+} signal	tropomyosin 1, regulates ca-dep interaction of actin- myosin, Myoferlin, Myoferlin	Tpm2 (3.60, 0.0035), MyoF (2.26, 0.0059), Myo1f (2.80, 0.0070)
Lipid	Phospholipase A2	Pla2g2a (2.53, 0.0084), Pla2g15 (1.77, 0.0075)
Cell cycle arrest & apoptosis	FBJ osteosarcoma viral oncogene homolog, pleiomorphic adenoma gene-like 1, lipocalin 2, lysozyme	fos (1.77, 0.0178), Plagl1 (3.49, 0.038), Lcn2 (4.14, 0.0029), Lyz2 (2.74, 0.0338)
Protein trafficking & phagosomal	RAS oncogene family, lysosomal/endosomal-associated membrane glycoprotein	Rab13 (1.90, 0.011), Rab32 (2.07, 0.0011), CD68 (3.69, 0.0003)
Metabolism	glutathione peroxidase 7, pyruvate dehydrogenase kinase, isozyme 2, hemochromatosis type 2, heat shock 70kDa protein 4-like, protein folding	Gpx7 (3.34, 0.0174), Pdk2 (-1.97, 0.0267), Hfe2 (-2.14, 0.026), Hspa4l (-1.67, 0.0365)
Mitochondrial activity	cytochrome b-245, NADH dehydrogenase (ubiquinone), GrpE-like 1, mitochondrial	Cybb (3.12, 0.0023), Ndufs4 (-2.26, 0.0157), Grpel1 (-1.69, 0.0274)
Fatty acid & cholesterol catabolism	peroxisomal membrane protein 2, apolipoprotein E	Pxmp2 (-1.77, 0.0347), ApoE (1.66, 0.0054)
Glucose transport	HtrA serine peptidase,may regulate insulin-likeGFs availability, insulin	Htra1 (3.36, 0.0244), Ins1 (-1.67, 0.0441)

Table 1: A list of genes whose expression is modified compared to sham upon MI only [FC> (+1.5) or FC< (-1.5), $p<0.05$] according to the gene chip array. Genes are affiliated with a specific KEGG pathway related to the cardiac structure or function. Only genes demonstrating best differential expression in the MI group relative to sham, are listed.

Gene Ontology	Gene Function	Gene Symbols (Fold-change STN vs Sham, p-value)
Ribosome biogenesis & translational elongation	ribosomal protein small subunits and basic leucine zipper, translational initiation	Rps14 (1.66, 0.018), Rps23 (1.73, 0.017), Rps19 (1.58, 0.030), Rps11 (1.61, 0.0187), Rps18 (1.52, 0.0243), Rps24 (1.61, 0.0441), Rps2-ps5(1.50, 0.0118), Rpl24 (1.52, 0.0484), Rpl37a (1.57, 0.0338), Rpl35a (1.5, 0.033),Bzw1 (-1.62, 0 .043)
Nucleosome assembly	histone 1 and histone 3	hist1h2bm (1.95, 0.045), hist1h2bf (1.54, 0.0331), hist3h2bb (1.64, 0.0355)
Ubiquitine-dependent proteolysis & catalytic actibity	proteasome subunit, ubiquitin specific protease, ubiquitin-fold modifier conjugating enzyme, RAS oncogene, may be involved in phagosome maturation, adaptor-related protein,protein lysosome targeting, N-glycanase (proteosome degradation of misfolded proteins), WAP four-disulfide core domain 2, protease inhibitor, phosphotriesterase related, catabolism	Psma3 (-1.52, 0.0152), Psma4 (-1.66, 0.0236), Psmd6 (-1.68, 0.0297), Usp16 (-1.52, 0.0484), Usp14 (-1.59, 0.0395), Ufc1 (-1.68, 0.0472), Rab14 (-2.12, 0.024), Rab2a (-1.73, 0.0263), Rab11a (-1.67, 0.0275), Rabif (1.59, 0.0299), Ap3m1(-1.98, 0.0198), Ngly1 (-1.56, 0.0272),Wfdc2 (-3.13, 0.0433), Pter (-1,54, 0.0467)
Lipid catabolism	phospholipase A2	Pla2g4c (-1.13, 0.0287
Proteolysis	mast cell protease, may be involved in cardiac hypertrophy	MCPT2 (-4.39, 0.0729*)
ER- Golgy transport	syntaxin, Golgi & post Golgy transport, endoplasmic reticulum aminopeptidase, vacuolar protein sorting 29, lectin, mannose-binding, involved in ER to Golgi transport	Stx7 (-1.86, 0.0333), Erap1 (-1.52, 0.0472), Vps29 (-1.88, 0.0348, Lman1 (-1.60, 0.0256)
Apoptosis	BCL2-like 13 (apoptosis facilitator), epithelial membrane protein 2	Bcl2l13 (-1.63, 0.0157), Emp2 (-2.18, 0.0491)
Inflammation	interleukin 13 receptor, lymphocyte antigen 6	Il13ra1 (-1.70, 0.0267), Ly6al (-1.98, 0.0518)
Transcriptional regulation & RNA processing	MAX interactor, myc transcriptional repressor, COMM domain, transcription regulator, RNA terminal phosphate cyclase, Cbp/p300-interacting transactivator, transcription coactivator	Mxi1 (-1.85, 0.0227), Commd3 (-2.01, 0.0231), Rtcd1 (-1.52, 0.0278), Cited4 (-1.73, 0.0480)
Protein folding	chaperonin containing TCP1, unfolded protein binding, t-complex, chaperon for actin & tubulin	Cct8 (-1.53, 0.0134), Tcp1 (-1.72, 0.0158)
Ca^{2+}-binding & cardiac contraction	scinderin, Ca(2+)-dependent actin-severing and -capping, calcium binding protein	Scin (-3.27, 0.0363), Chp (-1.57, 0.0255)
Adhesion, differentiation & cell growth	intercellular adhesion molecule 1, thioredoxin domain, acossiated with cell differentiation, secretoglobin, negative regulator of cell growth, ectonucleotide pyrophosphatase/phosphodiesterase 3	Icam1 (-1.51, 0.0358), Txndc9 (-1.61, 0.0323), scgb3a1 (-13.86, 0.0326), Enpp3 (-1.95, 0.0367)
Oxidation-reduction	selenoprotein, may be involved in oxidation-reduction reacts, isocitrate dehydrogenase 1 (NADP+)	Sepw1 (1.61, 0.0093), Idh1 (1.61, 0.0380)

Table 2: A list of differentially expressed genes (FC> +1.5 or FC< -1.5 and p<0.05), revealed from microarray experiment, that are affiliated with KEGG pathways specific to the cardiac structure or function, is presented (STN versus Sham) (important genes having exceptional p-values>0.05 are marked in a red asterisk). We selected genes demonstrating best differential expression in the STN group relative to sham. The turquoise highlight refers to genes whose relative expression was also tested by RT PCR; the green highlight demonstrates statistical significance in real-time analysis.

In the combined disease CRF (STN)+MI (Figure 4C) a significant downregulation in several ubiquinon biosynthesis genes including Coq2, Coq3, Coq6, Coq7 and Coq 10a was observed (Figure 4C and Table 2), pointing to a reduced energy-production mitochondrial activity of the failing heart. The decrease in the ubiquinone expression seems to be additive compared CRF or MI alone (Table 1 'Supplemental"). An RT analysis for a representative gene, Coq7, confirmed a significant downregulation compared to sham upon STN (-3.7, p< 0.001), MI (-2.5, p= 0.001) and to a greater extent upon STN+MI (-10.0, p<0.001). Furthermore, a significant induction in Notch3 was observed (though an RT analysis demonstrated a modest non-significant upregulation, Figure 5C), providing an additional evidence for the potential activation of Notch signaling in cardiomyocytes during post- MI remodeling [11]. In addition, a significant upregulation in the metalloproteinase MMP12 was noted in STN+MI both in the gene array and the RT analysis as documented in Figure 5C and Table 3. MMP12 elevation may mediate collagen degradation leading to LV dilation and ultimately heart failure, as previously demonstrated for other MMPs [12].

On an interesting note, one of the genes whose expression was significantly modified upon MI as well as CRF+MI, was the urine neutrophil gelatinase-associated lipocalin (Ngal) gene, LCN2 known to be associated with an acute idiopathic kidney injury [(+4.1, p=0.003 and +3.0, p=0.007 upon MI and STN+MI, respectively), Supplemental Table 1]. Upon the chronic state of STN only, Ngal levels remain unchanged (-1.4, p=0.17) in line with previous studies documenting that Ngal levels drop down when the renal injury becomes a chronic one [9]. In view of these data we thought to assess whether urine Ngal levels are indeed elevated upon acute MI and STN+MI. To this end we have utilized an ELISA for Ngal in rats' urine samples from groups corresponding to the ones used for the gene chip analysis: sham, STN (4 weeks post STN), MI (5 days post LAD ligation) and STN+MI. The data presented in Figure 5D represent mean values of 6 urine samples per each group. Notably, in line with the gene chip data, five days post acute MI or STN+MI, Ngal levels (720 ± 84 U/ml) were significantly higher compared to sham- operated animals (124 ± 40 U/ml) or the chronic STN animals (302 ± 157). Hence, in addition to confirming the Ngal gene expression data at the protein level, the Ngal ELISA readouts also point out to the potential use of Ngal as a diagnostic marker for renal injury resulting from an acute MI.

Discussion

The gross observations as well as the histological data and the gene chip array findings presented herein, strongly suggest that a major insult to the kidney enhances pathological changes in the heart, mainly

cardiac hypertrophy accompanied by interstitial fibrosis. Yet, the cardiac global systolic function remains unaffected.

We have also demonstrated that acute MI enhances a rapid moderate kidney injury as determined by Ngal levels five days post MI, both at the protein level (Ngal ELISA) and by the LCN2 gene chip data [13,14]. Using the gene chip array methodology, we have demonstrated that the vast majority of genes modified in the cardiac tissue upon CRF only- encode intracellular proteins, affiliated with cardiac hypertrophy. On the other hand the vast majority of genes modified upon MI or CRF+MI, are mainly translated to proteins affiliated with extracellular activity including matrix degradation, collagen deposition and focal adhesion.

It is already established that highly elevated urine Ngal readouts may indicate an acute kidney injury [15]. Several lines of evidence suggest that the detected Ngal upregulation in the mature kidney represents an intrinsic response of the kidney's proximal tubule cells to ischemic injury, which may be induced by local release of cytokines from neutrophils trapped in the microcirculation early after ischemic injury [16]. We thus conclude that apart from being a reliable early marker for acute kidney injury, urine Ngal could serve as a laboratory marker for short-term renal injury following acute MI. Urine Ngal could thus serve as a useful marker especially in intensive care units where ST-elevated myocardial infarctions as well as cardiogenic shocks are of everyday practice.

The observed cardiac hypertrophy and interstitial fibrosis occurring upon CRF may probably stem from both elevated preload and afterload in RF due to hypervolemia and increased peripheral vascular resistance respectively. Indeed, preload, induced by hypervolemia, causes serial addition of sarcomers leading to lengthening of myofibers and excentric hypertrophy, while increased afterload causes parallel addition of sarcomers, thickening of myofibers and concentric hypertrophy [17]. On the other hand, we should take into account when that infarction involves only or mainly the right ventricle, the left ventricular preload is actually reduced while the peripheral vascular resistance is increased in order to counter the systemic hypovolemia [18]. In this case we speculate that cardiac interstitial fibrosis would not be as high as in the LV MI model described here. An additional study has reported a significant increase in cardiomyocyte volume accompanied by a decrease of cardiomyocyte numbers per myocardial volume using a similar model for STN in rats [19]. Nevertheless, cardiac remodeling with interstitial fibrosis in patients with CRF is still poorly understood at the molecular level. Similarly, the uniqueness of genes and molecular pathways modified upon acute MI compared to CRF or combined disease is also poorly established. Yet, it is already recognized that cardiac hypertrophy, especially when diagnosed in the late stages of renal failure is one of the most important risk factors for acute MI, CHF and sudden cardiac death [20] as well as for renal deterioration requiring the use of dialysis [21]. In order to develop novel early biomarkers and potential pharmacologic approaches for left ventricular hypertrophy, it is necessary to recognize the genetic pathways leading to the dramatic changes in the tissue structure.

Amann et al. have previously presented gene chip array data, pointing to cardiac hypertrophy after STN as early as two weeks post surgery [22]. They have shown that genes encoding for collagens and proteoglycans are upregulated two weeks post surgery, and that 10

Gene Ontology	Gene Function	Gene Symbols (Fold-change and p-value)
Differentiation	notch 3, may be involved in cardiomyocyte differentiation, presenilin enhancer 2 homolog, required for the Notch signaling pathway	Notch3 (3.11, 0.0345), Psenen (-1.81, 0.0170)
Coenzyme Q biosynthesis	cytochrome c oxidase, coenzyme, required for Ubiquinone (coenzyme Q) biosynthesis, coenzyme	Cox18 (-2.04, 0.0036), Coq3 (-1.77, 0.0129), Coq7 (-1.74, 0.0063), Coq2* (-1.60, 0.057), Coq6 (-1.67, 0.026), Coq10a (-1.55, 0.013)
ECM proteolysis	matrix metallopeptidase 12, may have a role in glomerular injury, Disintegrin and metalloproteinase domain 12, ADAMTS-like 2	MMP12 (3.95, 0.0443), Adam12 (2.39, 0.0083), Adamtsl2 (1.66, 0.0073)
Cell migration	hyaluronan synthase	has1 (2.03, 0.0337)
Cell growth and proliferation	latent transforming growth factor beta binding protein 2, transforming growth factor b, early growth response 1, transcription, cyclin-dependent kinase 1, cyclin L2, EGF-like-domain, NDRG family member 3, negative regulation of cell growth	Ltbp2 (3.61, 0.001), TGFb1 (1.68, 0.0195), Egr1 (2.57, 0.0050), CDC2 (1.65, 0.0207), Ccnl2 (2.03, 0.0085), Egfl6 (-1.87, 0.0327), Ndrg3 (-1.80, 0.0091)
Ca-binding	transient receptor potential cation channel, subfamily V, member 2, two pore segment channel 1, Ca-channel activity	TRPV2 (1.66, 0.0035), Tpcn2 (1.56, 0.0341)
Transcription factors	nuclear transcription factor, nuclear receptor corepressor 2, transcriptional silencing, runt-related transcription factor	Nfxl1 (1.69, 0.0159), Ncor2 (1.51, 0.0209), Runx1 (2.13, 0.0314)
Proteolysis	mast cell protease 1, mast cell protease 10, mast cell protease 8	Mcpt1 (-2.20, 0.0495), Mcp10 (-1.87, 0.0221), Mcpt8 (-1.65, 0.0284)
Phagosome maturation	member RAS oncogene family	Rab20 (-2.09, 0.017), Rab27a (-1.61, 0.003)
Inflammation	interleukin 33, interleukin 17, interleukin 10	Il33 (-1.99, 0.0412), Il17ra (1.84, 0.0125), Il10ra (1.73, 0.0203)
Macromolecule metabolism Ribosome	aldehyde dehydrogenase 3 family, alcohol dehydrogenase 1A	Aldh3a1 (-1.61, 0.0135), Aldh3a2 (-1.53, 0.0273), Adh1 (-1.77, 0.0367)
Ribosome	ribosomal protein, exosome component 5, ribosome biogenesis	Rpl3 (1.88, 0.0254), Exosc5 (-1.57, 0.0481)

Table 3: A list of differentially expressed genes (FC> (+1.5) or FC< (-1.5), p<0.05), revealed from STN+MI treatment versus sham according to the gene chip array (Exceptional p-values are marked in asterisk). Genes that are affiliated with KEGG pathways specific to the cardiac structure or function are presented. Only genes demonstrating best differential expression in the STN+MI group relative to sham are listed. The turquoise highlight refers to genes whose relative expression was also tested by RT PCR; the green highlight demonstrates statistical significance in real-time analysis.

weeks later (12 weeks post surgery), a striking upregulation in laminins and integrins is noted. At our time point for animal termination (4 weeks and 5 days post STN surgery) neither one of these genes was modified in the cardiac tissue of the STN group. However, to the best of our knowledge we are the first ones to report an increase in numerous ribosomal genes as well as a decrease in proteolytic pathways, including pathways which are phagosome and complement-dependent. This tissue remodeling may induce endoplasmic reticulum stress as a response to an increased demand for protein synthesis as previously suggested [23]. The modification in the expression of these genes as well as the marked downregulation in several chymase genes point out to enhanced cardiac hypertrophy upon CRF.

Consequently, the gene chip data point out to a new set of biomarkers in the cardiac tissue which could indicate cardiac hypertrophy resulting from the various insults: 1. Upon CKD: downregulation of chymase genes and the complement factor C3 may probably reflect an inhibition

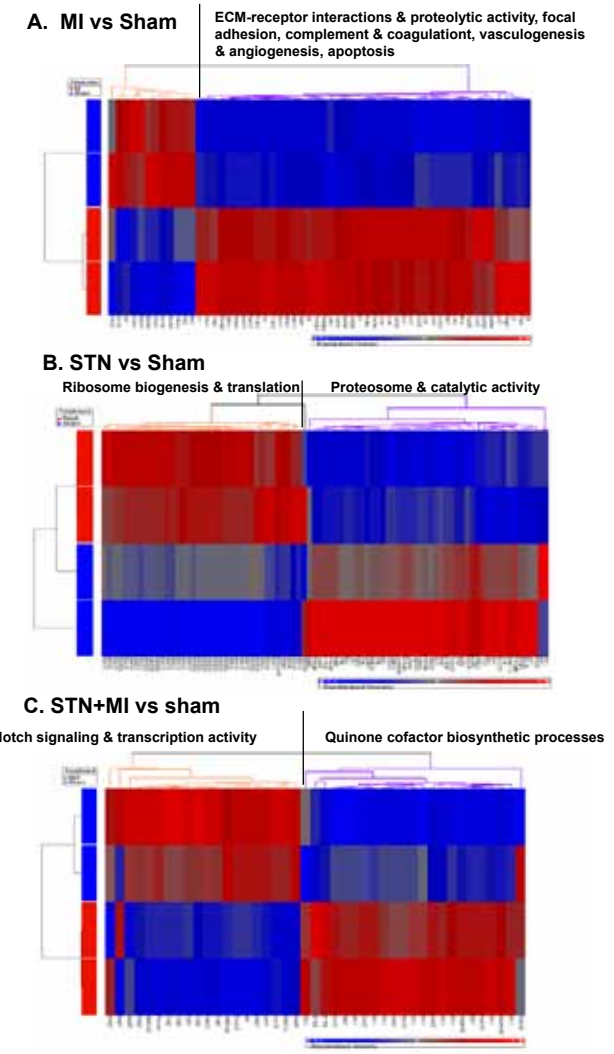

Figure 4: Functional annotations of clustered differentially expressed genes. An enriched functional annotation analysis of differentially expressed genes upon (A) MI, (B) STN, (C) STN+MI, each compared to sham, was obtained using the David software (http://david.abcc.ncifcrf.gov/tools.jsp). Hierarchical clustering show upregulated (red) or downregulated (blue) gene expression of the various treatments relative to sham.

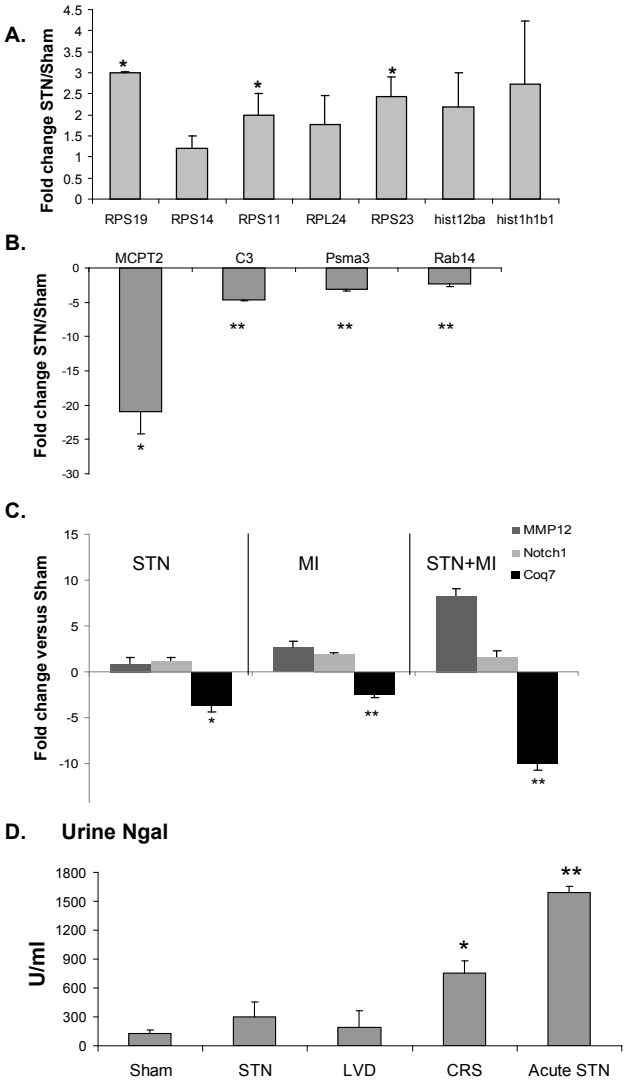

Figure 5: Real-time analysis. Validation analysis of several of the major interesting genes whose expression was modified in the gene chip array analysis compared to sham-operated controls (A) upregulated genes in STN versus sham-real time PCR (*) $p<0.05$ compared to sham; (B) downregulated genes in STN versus sham (real-time PCR) (*) $p=0.01$, (**) $0.05 < p < 0.01$; (C) genes modified in STN+MI compared to sham (real-time PCR) (*) $p< 0.01$ compared to sham, (**) $p< 0.001$ compared to sham; (D) Urine Ngal levels upon the acute and chronic insults (ELISA). (*) $p<0.01$ compared to sham, STN and LVD; (**) $p<0.01$ relative to sham, STN, LVD and CRS. The differences between readouts in panels A-C were tested by two-tailed student's t-test. The differences in the data depicted in panel D were analyzed by one-way ANOVA.

of cellular catalytic processes; an inhibition which is reversed upon acute MI, once removal of the necrotic cells becomes a must. 2. On acute MI: induction of several metalloproteinases could indicate early cardiac remodeling. It was previously suggested that MMPs could also serve as a prognostic marker in the circulation for cardiomyocyte injury and subsequent cardiac remodeling [12]. 3. In CRS- a marked downregulation in ubiquinon expression indicates that the cardiac metabolic function is severely damaged.

The ubiquinone which is also known as coenzyme Q is present in most eukaryotic cells, primarily in the mitochondria and serves

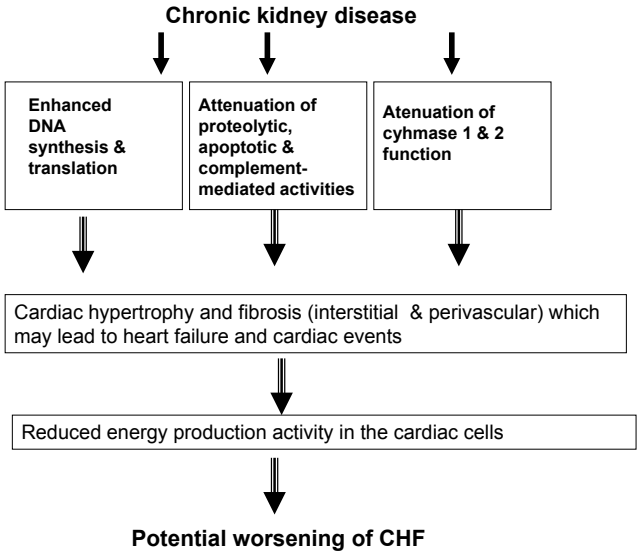

Figure 6: The potential molecular events leading to CRF and eventually to CRS.

as a critical component of the energy-generating electron transport pathways. Two additional studies have described a reduction in the expression of crucial mitochondrial components during the development of cardiac hypertrophy in rats or in human [24,25]. In line with these reports we demonstrate herein that these ubiquinone-forming genes are downregulated upon MI, upon STN only, and to a larger extent- upon CRS. The data may point to the potential therapeutic potential of Coq10 therapy for patients who are high risk for developing cardiac hypertrophy including conditions of CKD, CHF and above all, upon CRS.

As for the cardiac chymase expression, a previous biochemical study demonstrated that 24% of Angiotensin II (Ang II)- forming capacity in rat cardiac sections could be attributed to chymase-3 which converts Ang I to Ang II by cleaving the Phe8-His9 bond of Ang I. This activity was found to be chymostatin-inhibitable. On the other hand, β-chymases, i.e. rat chymases 1 and 2 were shown to be angiotensinases because they readily cleave the Tyr4-Ile5 and the Phe8-His9 bonds in angiotensins, thus degrading Ang I to inactive fragments [26]. Our data demonstrate modest downregulation in MCPT1 expression and a clear downregulation MCPT2 expression in the cardiac sections of STN compared to sham, while MCPT3 (chymase 3) expression remained unchanged. The data point out to downregulation of cardiac angiotensinase activity leading to enhanced formation of AngII, which is culminated in cardiac hypertrophy. Nevertheless, when considering the pathophysiological functions and possible therapeutic measures using chymase enzymes, we should take into consideration species differences in the enzymologic properties of the chymase. It should be noted that as opposed to the rat MCPT1 and 2 which degrade Ang I, the human chymase is known to be highly efficient at converting Ang I to Ang II [26]. A scheme illustrating the potential contribution of the identified pathways to cardiac hypertrophy and the ultimate progression to CRS is given in Figure 6.

Taken together, the understanding of CRF and CRS at the biochemical and the molecular levels may enable us to develop predictive biomarkers in the cardiac tissue, in the circulation or in urine samples. Furthermore, novel gene-based or pharmacological therapeutic modalities may emerge. Further studies are required in order to determine whether the modified gene expression observed at the RNA level also manifests at the protein level and to determine the appropriate required intervention with the ultimate goal of better identifying patients who are at increased risk for CRS complications including frequent hospitalizations and death.

Funding

The work was supported by the Israel Science foundation and by the Israeli chief scientist to G.K.

References

1. Ronco C, Haapio M, House AA, Anavekar N, Bellomo R (2008) Cardiorenal syndrome. J Am Coll Cardiol 52: 1527-1539.
2. Lekston A, Kurek A, Tynior B (2009) Impaired renal function in acute myocardial infarction. Cardiol J 16: 400-406.
3. Anavekar NS, McMurray JJ, Velazquez EJ, Solomon SD, Kober L, et al. (2004) Relation between renal dysfunction and cardiovascular outcomes after myocardial infarction. N Engl J Med 351: 1285-1295.
4. van Dokkum RP, Eijkelkamp WB, Kluppel AC, Henning RH, van Goor H, et al. (2004) Myocardial infarction enhances progressive renal damage in an experimental model for cardio-renal interaction. J Am Soc Nephrol 15: 3103-3110.
5. Windt WA, Henning RH, Kluppel AC, Xu Y, de Zeeuw D, et al. (2008) Myocardial infarction does not further impair renal damage in 5/6 nephrectomized rats. Nephrol Dial Transplant 23: 3103-3110.
6. Wong LS, Windt WA, Roks AJ, van Dokkum RP, Schoemaker RG, et al. (2009) Renal failure induces telomere shortening in the rat heart. Neth Heart J 17: 190-194.
7. Ben-Shoshan J, George J (2007) Endothelial progenitor cells as therapeutic vectors in cardiovascular disorders: from experimental models to human trials. Pharmacol Ther 115: 25-36.
8. Ben-Shoshan J, Schwartz S, Luboshits G, Maysel-Auslender S, Barzelay A, et al. (2008) Constitutive expression of HIF-1alpha and HIF-2alpha in bone marrow stromal cells differentially promotes their proangiogenic properties. Stem Cells 26: 2634-2643.
9. Nickolas TL, O'Rourke MJ, Yang J, Sise ME, Canetta PA, et al. (2008) Sensitivity and specificity of a single emergency department measurement of urinary neutrophil gelatinase-associated lipocalin for diagnosing acute kidney injury. Ann Intern Med148: 810-819.
10. Guo P, Hu T, Zhang J, Jiang S, Wang X (2010) Sequential action of Caenorhabditis elegans Rab GTPases regulates phagolysosome formation during apoptotic cell degradation. Proc Natl Acad Sci U S A 107: 18016-18021.
11. Oie E, Sandberg WJ, Ahmed MS, Yndestad A, Laerum OD, et al. (2010) Activation of Notch signaling in cardiomyocytes during post-infarction remodeling. Scand Cardiovasc J 44: 359-366.
12. Phatharajaree W, Phrommintikul A, Chattipakorn N (2007) Matrix metalloproteinases and myocardial infarction. Can J Cardiol 23: 727-733.
13. Ono K, Kuwabara Y, Han J (2011) MicroRNAs and cardiovascular diseases. FEBS J 278: 1619-1633.
14. Ding H, He Y, Li K, Yang J, Li X , et al. (2007) Urinary neutrophil gelatinase-associated lipocalin (NGAL) is an early biomarker for renal tubulointerstitial injury in IgA nephropathy. Clin Immunol 123: 227-234.
15. Grenier FC, Ali S, Syed H, Workman R, Martens F, et al. (2010) Evaluation of the ARCHITECT urine NGAL assay: assay performance, specimen handling requirements and biological variability. Clin Biochem 43: 615-620.
16. Mishra J, Ma Q, Prada A, Mitsnefes M, Zahedi K, et al. (2003) Devarajan P. Identification of neutrophil gelatinase-associated lipocalin as a novel early urinary biomarker for ischemic renal injury. J Am Soc Nephrol 14: 2534-2543.
17. Amann K, Rychlik I, Miltenberger-Milteny G, Ritz E (1998) Left ventricular hypertrophy in renal failure. Kidney Int Suppl 68: S78-S85.
18. Brookes C, Ravn H, White P, Moeldrup U, Oldershaw P, et al. (1999) Acute right ventricular dilatation in response to ischemia significantly impairs left ventricular systolic performance. Circulation 100: 761-767.

19. Amann K, Tyralla K, Gross ML, Schwarz U, Tornig J, et al. (2003) Cardiomyocyte loss in experimental renal failure: prevention by ramipril. Kidney Int 63: 1708-1713.

20. Wang AY, Li PK, Lui SF, Sanderson JE (2004) Angiotensin converting enzyme inhibition for cardiac hypertrophy in patients with end-stage renal disease: what is the evidence? Nephrology (Carlton) 9: 190-197.

21. Krishnan A, Oreopoulos DG (2007) Peritoneal dialysis in congestive heart failure. Adv Perit Dial 23: 82-89.

22. Amann K, Ridinger H, Rutenberg C, Ritz E, Mall G, et al. (2003) Gene expression profiling on global cDNA arrays gives hints concerning potential signal transduction pathways involved in cardiac fibrosis of renal failure. Comp Funct Genomics 4: 571-583.

23. Dickhout JG, Carlisle RE, Austin RC (2011) Interrelationship between cardiac hypertrophy, heart failure, and chronic kidney disease: endoplasmic reticulum stress as a mediator of pathogenesis. Circ Res 108: 629-642.

24. Li W, Rong R, Zhao S, Zhu X, Zhang K, et al. (2011) Proteomic analysis of metabolic, cytoskeletal, and stress response proteins in human heart failure. J Cell Mol Med 16: 59-71.

25. Weekes J, Wheeler CH, Yan JX, Weil J, Eschenhagen T, et al. (1999) Bovine dilated cardiomyopathy: proteomic analysis of an animal model of human dilated cardiomyopathy. Electrophoresis 20: 898-906.

26. Balcells E, Meng QC, Johnson WH Jr, Oparil S, Dell'Italia LJ (1997) Angiotensin II formation from ACE and chymase in human and animal hearts: methods and species considerations. Am J Physiol 273: H1769-H1774.